Spectro-Polarimetric Imaging for Object Recognition

L.J. Denes, M. Gottlieb, B. Kaminsky
Carnegie Mellon Research Institute
700 Technology Drive, Pittsburgh, PA 15230

D.F. Huber
Robotics Institute, Carnegie Mellon University
5000 Forbes Avenue, Pittsburgh, PA 15213

ABSTRACT

We have built an all-electronic spectro-polarimetric imaging camera utilizing an acousto-optic tunable filter and a liquid crystal variable retardation plate. This combination of rapidly adjustable parameters allows operation at 30/sec. frame rate, and near real time adaptability to changing target signatures. The spectral capability of the AOTF permits us to apply simultaneous, multiple wavelength filtering which greatly increases selectivity. Electronically agile polarization analysis adds a valuable signature feature for many scenarios. The adjustable retardation gives the capability to analyze and display not only linear polarization, but more generally, elliptical polarization as well. We have developed background suppression algorithms based on spectral and polarization signatures so that a wide variety of targets may be displayed with greatly enhanced contrast.

Keywords: multispectral imaging, spectro-polarimetry, acousto-optic tunable filter, target recognition

1. INTRODUCTION

Shape and spectral signature are well recognized identifiers in object recognition scenarios. Less well recognized is the importance of the polarization signatures from these objects. Objects often may reflect (or even emit in the infrared) radiation that has complex polarization content, depending upon their chemical composition or surface structure. Polarization content will be elliptical in general, the two extremes being circular and linear. The state of polarization can be completely characterized by the four components of the Stokes vector. Light reflected (or emitted) from man-made objects often differs from natural objects (i.e., vegetation, soil, rocks, etc.) in its polarization state. Therefore, polarization characterization may provide an additional discriminant where shape or simple color signature does not suffice to rapidly extract an object from its background.

We have applied spectro-polarimetric imaging techniques in two areas: target recognition military systems, and machine vision for transportation systems. For the first, we demonstrated the use of polarization signature as a means of enhancing the discrimination capability in friend-or-foe identification scenarios. For the second, we have developed and shown new processing algorithms for an autonomous vehicle testbed which will be used in driving scenarios, such as recognition of road signs, road hazards, road edges, and other vehicles. These projects have been carried out using a spectro-polarimetric imager that operates at high frames rates by combining an imaging acousto-optic tunable filter (AOTF) with an electronically controllable retardation plate (phase modulator). The choice of which method is used to implement the modulator will depend upon the spectral region to be covered, and the availability of suitable materials; several methods will be described in a later section. Such phase modulators can be switched to any random retardation on a short (millisecond or less) time scale. It is this agility together with the agility of the AOTF that makes the spectro-polarimetric imaging concept useful in applications requiring high data rates. Our current imaging AOTF spectro-polarimeter operates from 0.5 to 1 micrometer by combining an AOTF with a liquid crystal electronically variable retarder, both under computer control. However, it is in the infrared rather than the visible where the greatest potential for exploiting complex (i.e., elliptical) polarization signatures lies to enhance discrimination. Present systems are limited in their IR range to 4.5

micrometers by the AOTF crystal (tellurium dioxide) transmission limit and the liquid crystal variable retarder can operate to only 1.8 micrometers. In order to overcome this lack of the required IR devices, we are developing AOTFs based on mid-IR crystals grown at our laboratory, and a custom designed and fabricated ZnSe photo-elastically variable retardation plate.

2. MULTISPECTRAL IMAGING

Spatial characteristics have been the dominant discriminant in object recognition studies, but it has been firmly established that spectral filtering has an important role to play in many applications of object identification. Multispectral filtering has already been widely used for many years in remote sensing systems, typically using fixed, wideband pass filters. Color cameras are of limited use for analyzing color content of objects in a scene because the sensitivity curves for each of the RGB components include a wide spectral range, resulting in low specificity. Current 2-D spectral imaging systems typically utilize fixed filters that are rotated into place, and are speed limited by mechanical factors. Advanced spectral imaging technology will require that detailed spectral data be acquired at high rates and with good accuracy. The acousto-optic tunable filter is limited in its speed by acoustic transit times across the device, typically less than 30 microseconds per spectral sample, and spectral resolution is on the order of 1% of center wavelength, and is electronically adjustable. For the range from 0.4 to 1.0 micrometers, this yields about 100 resolution elements.

Using multispectral imaging, military target vehicle signatures may be adequate for positive identification under a wide range of field conditions. Greater security can be achieved by applying "tags" on friendly vehicles which produce unique signatures in the IR but which, in the visible, may appear as camouflage paint. Such tag paints are modified formulations of conventional camouflage paint. Because the AOTF is electronically programmable, stored signatures can be rapidly changed on-line. A unique capability of the AOTF is its ability to perform simultaneous multi-spectral filtering; i.e., it may be operated to transmit several wavelengths simultaneously in order to closely simulate a complex spectral signature with far greater discrimination than can be achieved with a single passband. Since most objects of interest exhibit such complex spectra, the AOTF can greatly enhance the identification process.

Promising applications of multispectral imaging exist in vehicle control systems, such as detection and reading of road signs, and location of road boundaries and other distinguishing road features. As an example, we have developed a vegetation detection algorithm that is useful for off-road navigation as part of a larger effort to develop a terrain classification module[1]. Present capabilities preclude easily distinguishing between rocks, tall grass and low shrubs and features[2]. Better object classification will reduce the number of false positives for obstacles. Intensity-based terrain classification with black and white camera is difficult because different features may produce similar intensities, and because of the great relative intensity variation for different light conditions. Color cameras are helpful, but various features typically appear only in dull shades of green and brown. However, more complete spectral analysis reveals better spectral signatures, such as that due to the large chlorophyll reflectance of plants in the 690 to 730 nm range. We have taken spectral scans of road and nearby brown (winter) grass with the AOTF analyzer in the visible range as shown in figure 1 where this spectral peak is easily seen. Trees and other flora also show other distinct spectral signatures[3].

Our algorithm uses the ratios of intensities in this band by operating the AOTF in a rapid switching model. This technique is relatively insensitive to varying lighting conditions, performing well in sunny, partly cloudy and overcast conditions.

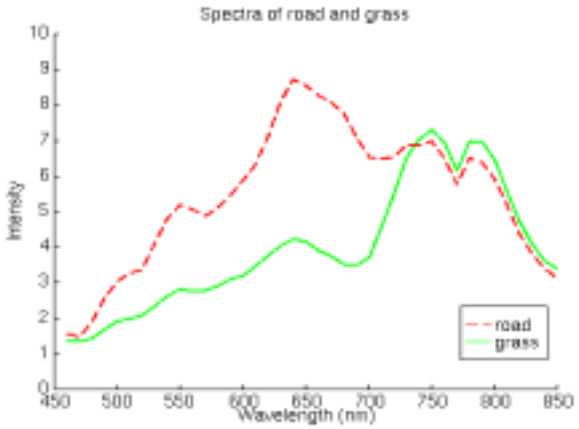

Fig. 1. Example of a typical spectra of brown grass in winter and gray road surface. The grass shows a marked peak between 700 and 850 nm

3. POLARIZATION ANALYSIS

Polarimetry is a well established tool in a variety of systems for enhancing visibility of objects. For example, differentiating surfaces by effects of specular and diffuse reflection, edge identification between objects and background and discrimination between metal and dielectric surfaces. The latter is a result of the characteristic elliptical polarization produced by metal surface reflection. It is also well known from common remote sensing experience that soil and rocks tend to strongly polarize light while grass does not. In a typical military situation involving camouflage, in which camouflage netting is colored and textured to visually resemble the background, the netting can be discriminated by its high polarization of reflected light as compared with background terrain. Another such prominent feature is due to the antiballistic glass used on military vehicles, for which light transmitted through the glass exhibits much different polarization. In satellite monitoring systems, polarization is an excellent indicator of atmospheric particle and aerosol size and cloud particle size distribution. Circular polarization may be produced by certain types of foliage due to the birefringence sometimes present in floral structures. Circular polarization is relatively infrequent in nature, and its analysis will require incorporating 1/4-wave plates into the polarimetric system as well as linear polarizers. However, it can add an additional powerful discriminant to define the signature.

The polarization composition of light from a scene is represented by using the Stokes parameters, I, Q, U, and V, that make up the Stokes vector. These four quantities are the time averages of various combinations of two orthogonal amplitudes of the electric field I_X and I_Y and the phase angle γ between them. They are defined as:

$$I = \langle I_X^2 + I_Y^2 \rangle \quad . \tag{1}$$

$$Q = \langle I_X^2 - I_Y^2 \rangle \quad . \tag{2}$$

$$U = \langle 2 I_X I_Y \cos\gamma \rangle \; . \tag{3}$$

$$V = \langle 2 I_X I_Y \sin\gamma \rangle \; . \tag{4}$$

These quantities are physically the intensity, I; the plane of polarization, Q; the excess of plane polarization at +45•, U; the amount of circular polarization, V. The percentage of plane polarization, P, is defined as:

$$P = 100 \times (Q/I), \tag{5}$$

which is calculated directly from the intensity measurements. The phase angle, γ, requires the use of a 1/4-wave plate (or retardation plate) in conjunction with a linear polarizer in order to convert the phase angle measurement to a simple

intensity measurement. The 1/4-wave plate is generally made from a birefringent crystal such as calcite, with ordinary refractive index, n_o and extra-ordinary index, n_e, and accurately polished to a thickness L so that when light of wavelength λ passes through the crystal the components of the light polarized parallel to the ordinary and extra-ordinary axes of the retardation plate will experience a relative phase difference of •/2 radians. The phase delay, •Ø , governing this process is:

$$•Ø = 2•L(n_e-n_o)/\lambda = •/2 . \qquad (6)$$

The method by which this converts circular to linear polarization is by rotation of direction of one component by 90°. The 1/4-wave plate is specific to each wavelength once n_e, n_o and L are specified; thus, every element of wavelength requires its own plate. A complete analysis of a scene therefore requires either a set of fixed retardation plates or one variable plate. Single achromatic plates have been designed but are very difficult to implement, especially in the infrared, because they require extremely high tolerances on refractive indices, thickness, and high temperature stability. For example, four decimal place refractive index accuracy, and one micrometer thickness accuracy are typical for the important 3 to 5 micrometer range. For these reasons, electronically variable retardation plates are needed to operate spectro-polarimetric imaging systems at video frame rates.

Most polarimetric measurements for determining the Stokes parameters utilize either quarter-wave plates mechanically rotated at a fixed rate with measurement of the DC component, first and second harmonics of the detected signal, or just performing intensity measurement with different orientations of the quarter-wave plate[4]. Neither of these methods can be applied for image polarimetry in near real time. The theoretical analysis of light of arbitrary polarization passing through a system of two phase modulators and a linear polarizer has been carried out[5]. We have applied this analysis to processing images with complex polarization . The first phase modulator with axis K and K' produce phase shift δ_1, and the second phase modulator with axis f (ordinary) and s (extraordinary) produce phase shift δ_2. For simplicity, let us choose the x and y directions to lie along the large and small axes, respectively, of the polarization ellipse of the incident light, as shown in figure 2.

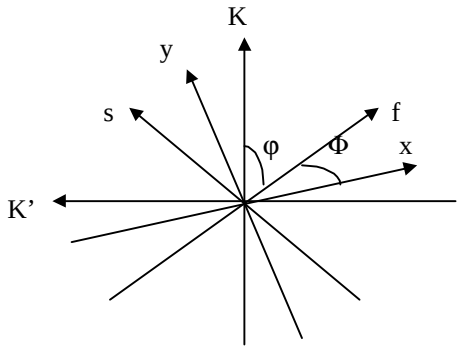

Fig. 2. Coordinate system for polarization analysis

The angle between the ordinary axis of the second phase modulator and the x axis is denoted by Φ, the angle between the axes of the first and second phase modulators is φ. The axis of the analyzer (not shown in figure 2) is at an angle of 45° to the first phase modulator axis. In such coordinate system U ≡ 0 and Φ is the angle between the major axis of the ellipse and the axis of the second phase modulator. As shown in reference 5, the intensity of light leaving the analyzer I_a (assuming that U ≡ 0) is calculated as:

$$I_a = 0.5 [I - Q (\cos(2\Phi) \sin(2\varphi) \cos\delta_1 + \sin(2\Phi) \cos(2\varphi) \cos\delta_2 \cos\delta_1 - \\ - \sin(2\Phi) \sin\delta_2 \sin\delta_1) - V (\cos(2\varphi) \sin\delta_2 \cos\delta_1 + \cos\delta_2 \sin\delta_1)]. \qquad (7)$$

Now, let us consider four different cases.

1) Let $\delta_1 = 0$, $\delta_2 = 0$

$$I_a = 0.5 [I - Q \cos(2\Phi) \sin(2\varphi)] . \qquad (8)$$

2) Let $\delta_1 = 0$, $\delta_2 = \pi / 2$

$$I_a = 0.5 [I - Q \cos (2\Phi) \sin (2\varphi) - V \cos (2\varphi)] . \quad (9)$$

3) Let $\delta_1 = \pi / 2$, $\delta_2 = 0$

$$I_a = 0.5 [I - V] . \quad (10)$$

4) Let $\delta_1 = \pi / 2$, $\delta_2 = \pi / 2$

$$I_a = 0.5 [I - Q \sin (2\Phi)] . \quad (11)$$

From the equations (8) - (11) the values of I, Q, V, and Φ can be determined. For totally linear polarized light when $U \equiv 0$

$$I^2 = Q^2 + V^2 . \quad (12)$$

For partially polarized light the percentage of plane polarization, P, is evaluated from the formula:

$$P = (Q^2 + V^2)^{1/2} / I . \quad (13)$$

The overall image area can be divided into subareas where we can assume the state of polarization is uniform. Using equations (8) - (11) the Stokes parameters can be calculated for such subareas and used for further image processing like separation between linear and ellipticallly polarized radiation (by the value of the parameter V) or between different orientations of the linear polarized light (by the value of the parameter Φ). For the AOTF camera system the AOTF itself serves as analyzer. If liquid crystal variable retardation plates are used as phase modulators, the transition between cases 1 - 4 described above can be achieved within typically 20 msec and the processing of the whole image can be done within 100 msec.

4. AOTF/POLARIMETER CAMERA SYSTEM

4.1 The Acousto-optic Tunable Filter

The AOTF was invented by Harris[6] in 1969, and extensively developed more recently as an imaging device. It consists of a transparent crystalline material [7] typically one cubic inch in size, with an acoustic transducer plate bonded to one face. A radio frequency signal, usually in the range from 10 to 100 MHz, is applied to the transducer, which generates an acoustic wave that propagates in the crystal. The acoustic wave in the crystal modulates the refractive index, thereby selectively diffracting incident light according to its wavelength, and the value of the RF. A typical device configuration is illustrated in figure 3.

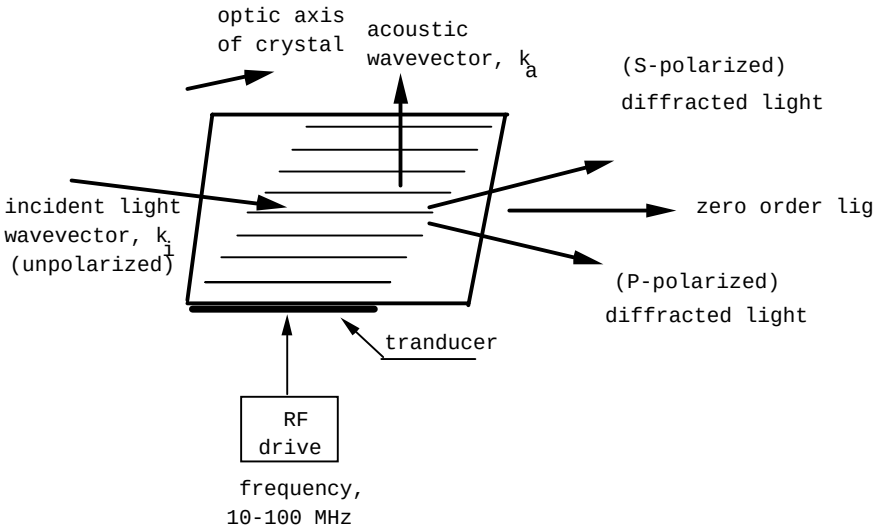

Fig. 3. Typical AOTF configuration

Changing the radio frequency, f, will vary the modulation spacing (phase grating spacing) and the wavelength, λ, of light selected for diffraction. The relation between these is

$$f = K/\lambda \,, \qquad (14)$$

where K depends upon the intrinsic properties of the crystal material, and its angular orientation. An important feature of the AOTF diffraction process is that the filtered (i.e., diffracted) light is separated spatially from the incident beam. In addition, the filtered beam is divided into its two orthogonally polarized components, as shown in the figure 3.

4.2 The Variable Retardation Plate

The techniques of analyzing polarized radiation using various combinations of linear polarizers and retardation plates are well known[8]. The intensity of circularly polarized light can not be made subject to intensity variation by rotating a linear polarizer. The retardation plate modifies the state of polarization of the light as it passes through, so that a linear polarizer may subject it to intensity variation for visualization. However, each retardation plate for 1/4-wave is specific to the wavelength from eq. (6), as dictated by its thickness and refractive indices. Thus each wavelength requires a different plate, so that a complete polarization analysis of a scene would require a complete set of retardation plates. These would have to be sequentially positioned in the spectral imaging system, as each wavelength was addressed. Consequently, the rate at which data could be accumulated would be unacceptably slow for most applications.

The process of accumulating spectro-polarimetric imaging data can be operated at high rates by combining the imaging AOTF system with an electronically controllable retardation plate, which we refer to as the phase modulator. Means to implement such a phase modulator include such physical effects as electro-optic modulation and photo-elastic modulation. With these effects, the refractive indices and the birefringence $n_e - n_o$ are made to vary in response to an electrical signal. According to equation (6), the quarter wave relationship for a fixed L can be made for varying λ by applying an electrical signal so that $(n_e - n_o)$ will satisfy (6). In general, the modulator should be capable of +/- π radian change to map the entire polarization space. While this is relatively easily done at short wavelengths in the visible, it becomes increasingly difficult at long wavelengths in the infrared, since very large changes in $(n_e - n_o)$ may be required.

The phase modulation method chosen will depend upon the wavelength range of operation, UV, visible, near infrared or far infrared. For the visible and near infrared range, liquid crystal electronically variable retardation plates along with their

electronic controls are commercially available and are relatively inexpensive. For the UV and visible, variable retardation can be implemented with an electro-optically controlled crystal, such as KDP or lithium niobate. A schematic of an electrooptical retardation modulator is illustrated in figure 4.

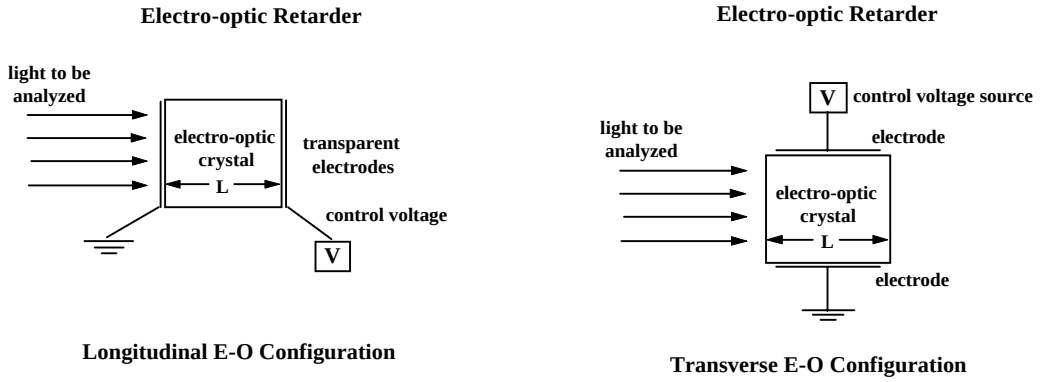

Fig. 4. Electro-optically controlled variable retardation plate

In this type of modulator, the refractive index and birefringence are functions of the electrical field, E. For the mid-infrared and far-infrared, materials are available for a photo-elastic phase modulator. For this type, the refractive index and birefringence is determined by the amount of applied uni-axial pressure and its direction. The compression may be varied electronically by means of a piezo-electric stack mounted in contact with the modulator plate. Favorable materials for the infrared include germanium, silicon and zinc selenide. The voltage applied to the piezo-electric stack will govern the compression, and therefore the birefringence and retardation wavelength of the plate. Switching can be done on this at millisecond rates.

4.3 The Camera System

The AOTF imaging system is shown schematically in figure 5, and the optical head for our prototype system is shown in the photograph figure 6.

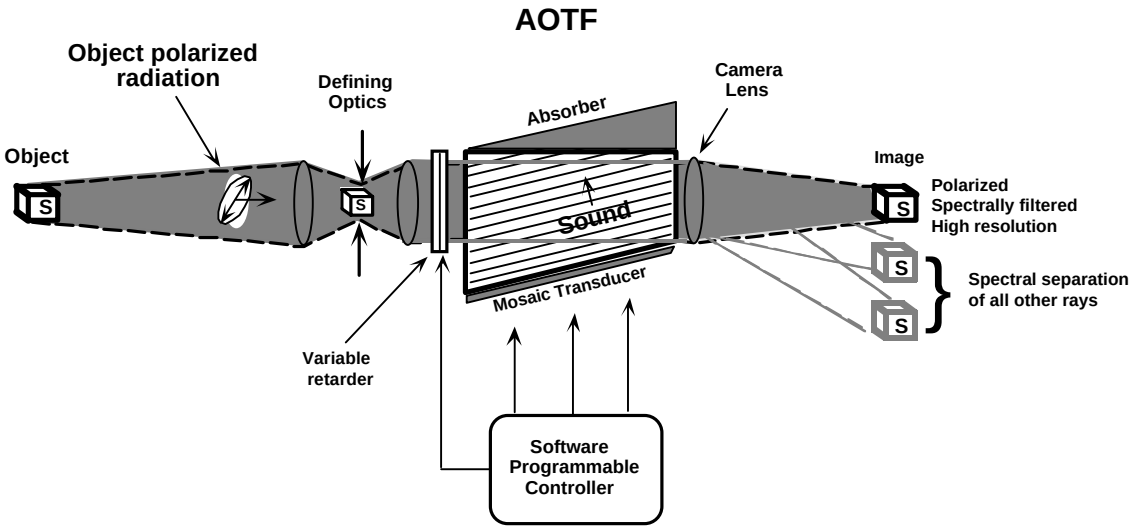

Fig. 5. Schematic of AOTF camera system.

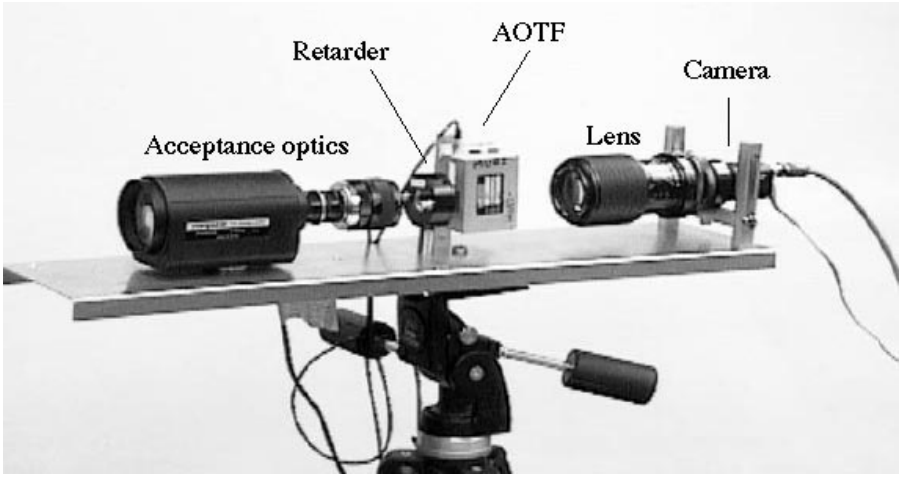

Fig. 6 Prototype spectro-polarimetric system optical head

Because the filtered image contains only a small fraction of the incoming light, its acquisition requires a high sensitivity, low noise focal plan array camera. We use a Watec WAT-902A CCD camera that features a signal to noise ratio of 46 dB, sensitivity of 0.05 lux at f/1.2, and a 30/second frame rate. The camera is interfaced with a PCI-based frame grabber board (ImageNation PX500) for real time image processing. The AOTF can be driven by a variety of RF sources, depending upon the desired operational mode: arbitrary waveform generator (Tektronix/SONY AWG2040) for maximum flexibility, a single VCO for sweep mode to perform complete spectral scans, or several switchable oscillators for maximum speed and simplicity. The arbitrary waveform generator AWG2040 features a sampling speed of one giga samples per second and a one megabyte memory for the waveform storage with 8 bit data length. The unit communicates with the host computer via IEEE488 bus. The output of the generator drives a one Watt wide band amplifier, which is split into three and fed into three transducers via an impedance matching network. The arbitrary waveform generator affords us a high degree of scenario selection to drive the AOTF. For example, waveforms that achieve multiple passbands and a spread spectrum can be easily programmed. However, in many applications, desired effects may be obtained simply by switching between sinusoidal waves of selected frequencies. Such control functions may be implemented using a voltage controlled oscillator and a computer controlled D/A converter. The retarder voltage is controlled digitally using the unit supplied by the manufacturer

A background suppression algorithm was developed to optimize the contrast of signature targets in the presence of high levels of clutter. This algorithm utilizes a software mask which is generated in near real time. The steps in the algorithm are illustrated in figure 7, in which a simulated battle scene was created with variously colored objects, including two tanks painted with slightly different colors (signature and non-signature spectra), vegetation, sand and water. The software mask is created by recording the scene at a non-signature wavelength and inverting the intensities to create a negative of the scene. The mask is then subtracted from the scene taken at the signature wavelength, and the product subjected to a threshold subtraction, leaving only the target above a dark background.

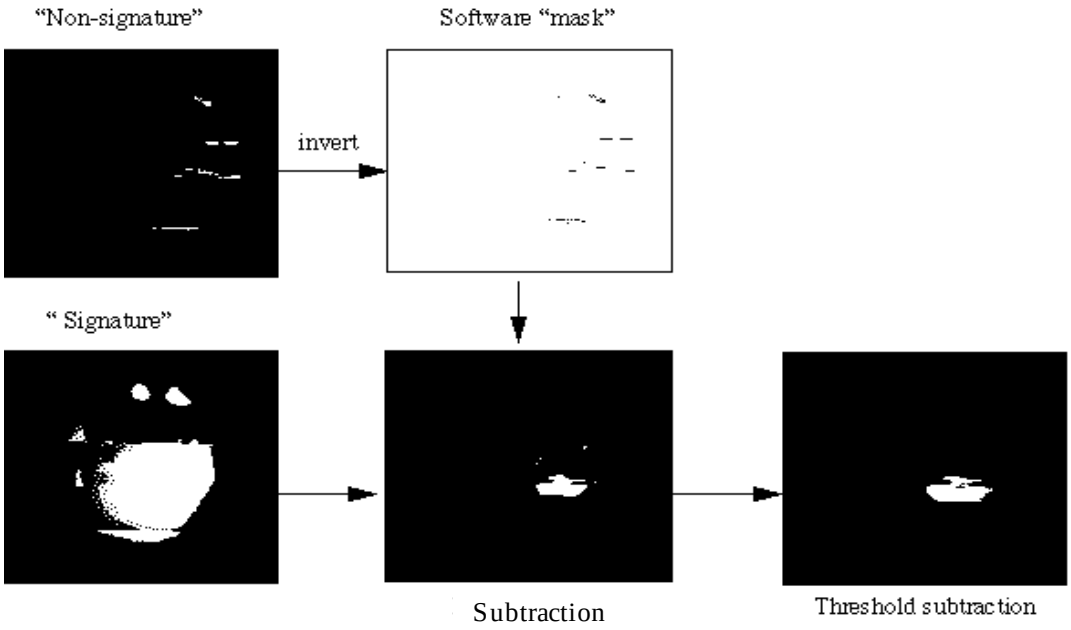

Fig. 7 Procedure for background suppression with target signature software mask

5. EXAMPLES OF TARGET RECOGNITION with SPECTRO-POLARIMETRIC IMAGING

The system was applied to a laboratory demonstration of camouflaged target extraction from a battle scene scenario, as illustrated in figure 8.

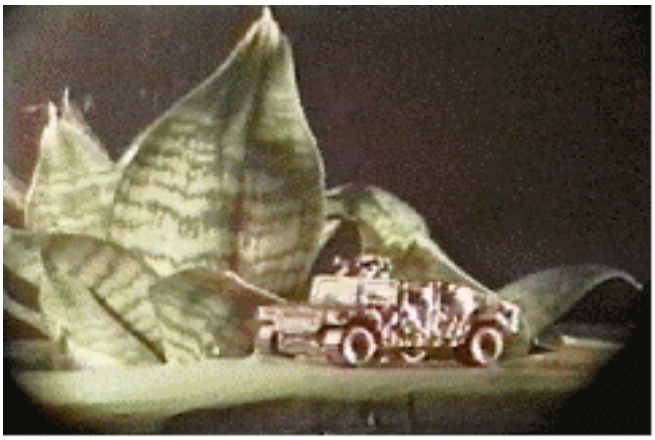

Fig. 8 Unfiltered simulated battle scene with target vehicle

The scene was constructed using a model of a military vehicle painted with actual camouflage paint, placed near live vegetation of similar color. The scene filtered in the green through the AOTF system gave maximum intensity to the vehicle, but also to the vegetation. Thus, color alone gives insufficient discrimination for the target. Discrimination is greatly enhanced by using the difference in polarization of the light reflected from vehicle and background vegetation. Measurements were done with the spectro-polarimeter at a wavelength of 633 nm, varying the voltage on the liquid crystal retarder to span 2π radians of retardation. The intensities for two 4x4 pixel areas, one from the vehicle image and the other from the vegetation image, are compared in figure 9.

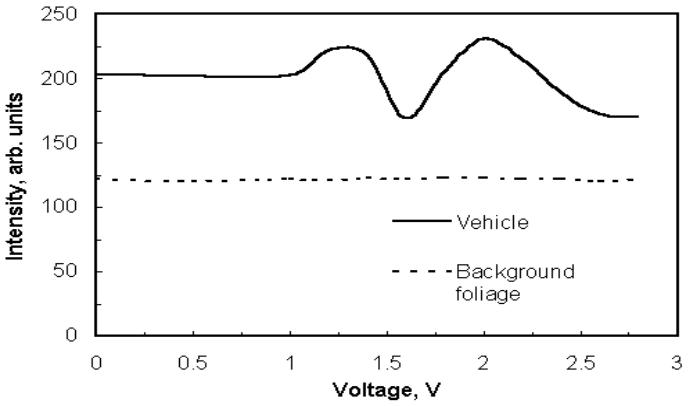

Fig. 9. Modulation of intensity of typical 4x4 pixel area from target vehicle compared with background foliage with change of retardation plate voltage

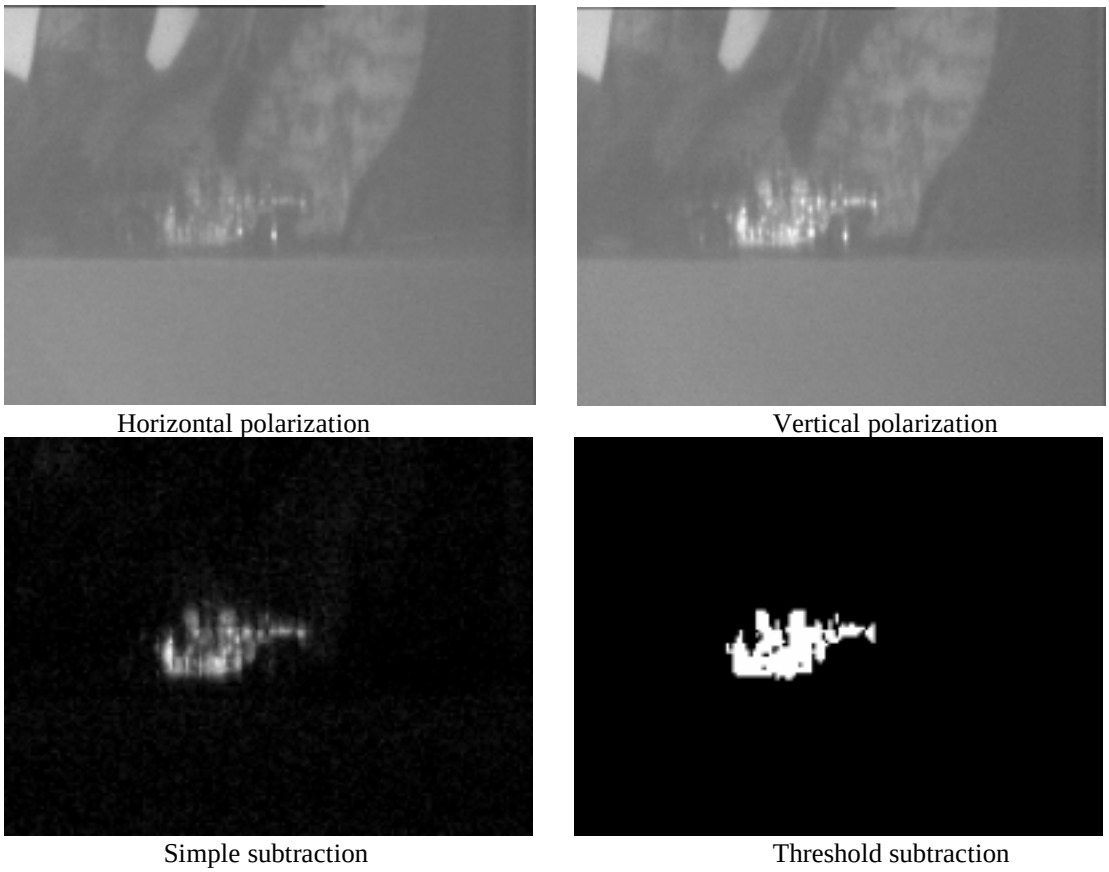

Fig. 10. Background suppression procedure applied to polarimetric target image

The target shows about a 30% intensity modulation with varying retardation, while the vegetation shows almost none. We applied the same background suppression algorithm to this scene, using the target polarization signature rather than the spectral signature to create the masks. The results are shown in figure 10 for the different steps in the process. While the polarization filtering alone already greatly improves the contrast against background, the subtraction and threshold processing adds many levels of additional discrimination. The system was applied to an outdoor scene to demonstrate its capabilities for a road hazard detection scenario, glare detection from wet or icy surfaces. Glare detection is accomplished by processing the horizontally and vertically polarized images taken switching the retardation plate between the two so as

to extract the minimum and the maximum intensity images. These two frames can then be subtracted and thresholded to highlight the highly polarized regions. The steps of the algorithm applied to the wet road scene are shown in figure 11.

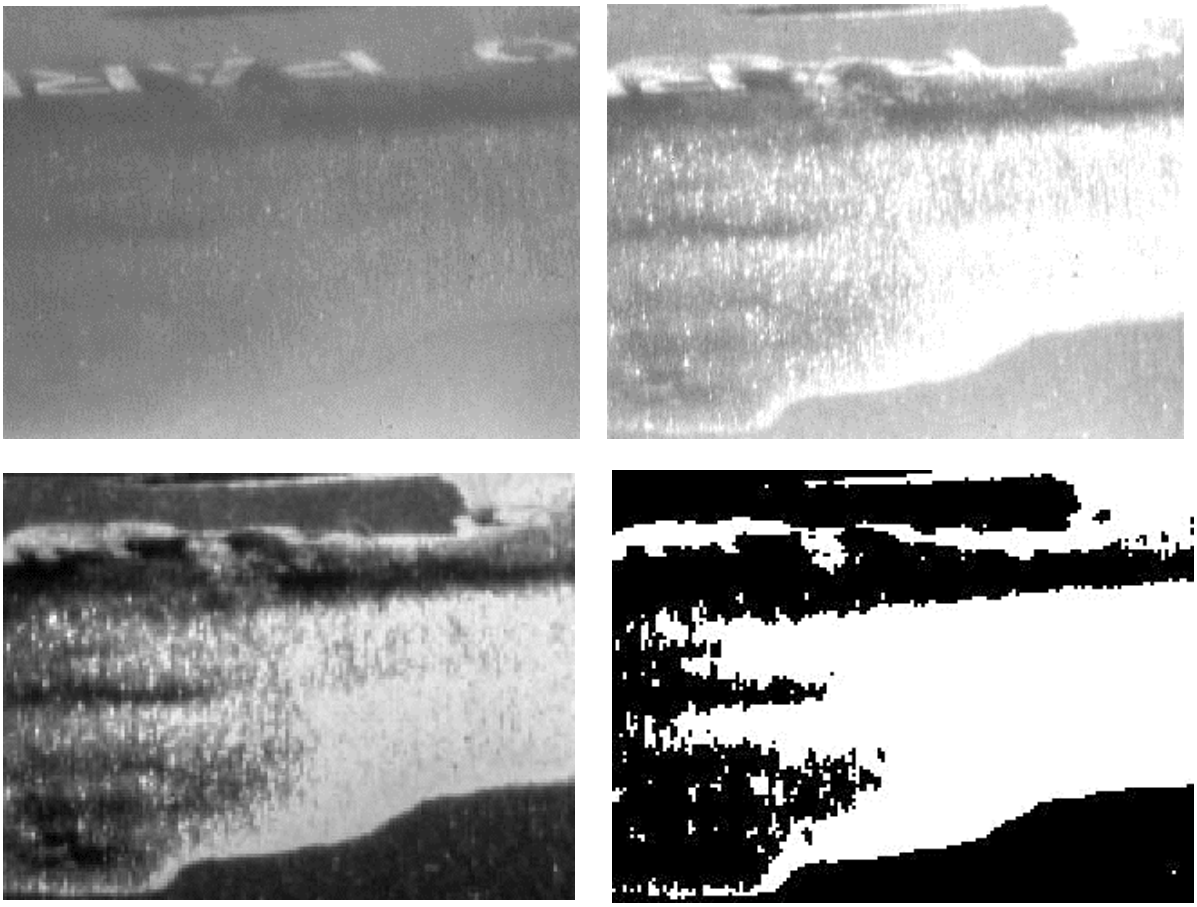

Fig. 11. Wet road polarization detection. Top row: original images of partially wet road with retarder for minimum and maximum intensities. The top center and left and bottom right areas of the scene are dry. Bottom row left: scene processed to emphasize contrast between dry and wet pavement. Bottom row right: the enhanced image thresholded to identify high glare (wet) regions. Notice that areas with high reflectance and no glare, such as the stem of the letter P, are correctly identified as having no glare.

6. CONCLUSION

The performance of image recognition system can be greatly improved by incorporating the capabilities for multispectral and polarimetric analysis. We have accomplished this objective by using an AOTF-based camera system to which we have added electronically variable retardation plates. These are well suited to many systems requiring operation in an adaptive fashion, and at high random access rates. Adaptability is especially important in tactical situations where designated targets may be changed frequently. All-electronic systems, such as the AOTF polarimeter, can be changed with only software, keeping the hardware in place. We have demonstrated the use of the system for such military applications as camouflaged target detection and friend or foe identification, as well as for vehicle vision applications, such as determination of road conditions. These demonstrations were in the visible, but it is anticipated that multispectral polarization analysis would be even more useful in the infrared. We have developed system designs for extending these concepts to the 3 to 5 and the 8 to 11 micrometer spectral ranges.

7. ACKNOWLEDGMENTS

This work was supported under the U.S. Navy contract No. NOOO14-95-1-0591. The views and conclusions contained in this document are those of the authors and should not be interpreted as representing the official policies, either expressed or implied, of ONR or the U.S. Government.

8. REFERENCES

1. I.L. Davis, A. Kelly, A. Stentz, and L. Matties, "Terrain Typing for Real Robots", Proc. of the Intelligent Vehicles "95 Symposium, Detroit, MI, Sept. 1995, pp. 400-405.
2. M.H. Hebert, C. Thorpe, and A. Stenz, eds., Intelligent Unmanned Ground Vehicles - Autonomous Navigation Research at Carnegie Mellon, Kluwer, Boston, 1997.
3. W. G. Egan, "Polarization in remote sensing", Proc. S.P.I.E., **1747**, 2 (1992).
4. D. Clarke and J.F. Grainger, "Polarized Light and Optical Measurement", Pergamon Press, (1971).
5. B.A. Ioshpa and V.N. Obridko, (Photoelectric analysis of polarized light", Optics and Spectroscopy, **15**, 60 (1963).
6. S.E. Harris and R.W. Wallace, "Acousto-optic tunable filter", J. Opt. Soc. Am., **59**, 744-747, (1969).
7. M. Gottlieb, "Materials for AOTF", in "Design and Fabrication of Acousto-optic Devices", ed. A.P. Goutzoulis and D. R. Pape, chap. 3, Marcel Dekker, Inc. (1994).
8. F.A. Jenkins and H.E. White, "Fundamentals of Optics", chap. 27, McGraw-Hill (1957).